Original Article

# Three Methods Assessing Red Marrow Dosimetry in Lymphoma Patients Treated With Radioimmunotherapy*

Ludovic Ferrer, MS[1,2]; Françoise Kraeber-Bodéré, MD, PhD[2,3,4]; Caroline Bodet-Milin, MD[2,4]; Caroline Rousseau, MD[2,3]; Stephen Le Gouill, MD, PhD[2,5]; William A. Wegener, MD, PhD[6]; David M. Goldenberg, MD, PhD[7]; and Manuel Bardiès, PhD[1,2,3,4]

**BACKGROUND:** Maximum injected activity in radioimmunotherapy (RIT) is limited by bone marrow toxicity. Many dosimetric approaches have been proposed, leading to high variability in the results and elusive absorbed dose-effect relations. This study presents the results of red marrow (RM) absorbed dose estimates performed with 3 methods. **METHODS:** Five patients received 2 co-infusions of $^{90}$Y-labeled (370 MBq/m2) and $^{111}$In- labeled (120 MBq) epratuzumab (1.5 mg/kg) 1 week apart. RM-absorbed dose was estimated by 3 methodologies. The first approach (M1) used $L_2$-$L_4$ lumbar vertebrae imaging. M2 and M3 methods used different red marrow to blood ratios (RMBLR) to assess RM-absorbed dose. RMBLR was set to a fixed value of 0.36 in M2 or assessed according to each patient's hematocrit in M3. **RESULTS:** Median RM-absorbed doses were 4.1 (2.9-8.4), 2.3 (2.0-2.7), and 2.3 (1.6-2.5) mGy/MBq for M1, M2, and M3, respectively. No trend could be found between total RM-absorbed dose and toxicity for M2 and M3. Conversely, M1 seemed to provide the best absorbed dose-effect relation. The 4 patients with the highest RM-absorbed doses exhibited grade 4 toxicity. The fifth patient, with the lowest RB absorbed dose, exhibited only a mild (grade 2) toxicity. **CONCLUSIONS:** Image-based methodology (M1) seems to better predict hematological toxicity as compared with blood-based methods. Only this method provides for bone marrow involvement. ***Cancer*** **2010;116(4 suppl):1093–100.** © *2010 American Cancer Society.*

**KEYWORDS:** radioimmunotherapy, red marrow dosimetry, epratuzumab, yttrium-90, CD22.

**Radioimmunotherapy** (RIT) is a new modality of targeted therapy in which radiation from radionuclides is delivered more selectively to tumor using monoclonal antibodies directed to tumor-associated antigens. Today, RIT can be used in clinical practice with nonmyeloablative administrations of murine anti-CD20 $^{131}$I-tositumomab (Bexxar, GlaxoSmithKline, Philadelphia, Pa) approved in the United States, and with $^{90}$Y-ibritumomab tiuxetan (Zevalin, Cell Therapeutics, Seattle, Wash; Bayer Schering Healthcare, Berlin, Germany, approved in Europe and in the United States for treatment of patients with relapsed or refractory follicular lymphoma.[1,2] Other antibodies, such as the humanized anti-CD22 $^{90}$Y-epratuzumab tetraxetan, are in clinical development.[3-8] $^{90}$Y-epratuzumab tetraxetan is a promising RIT agent because it is humanized, internalized by target cells, and stably labeled using tetra-azacyclododecanetetra-acetic acid (DOTA). Moreover, contrary to $^{90}$Y-ibritumimab tiuxetan or $^{131}$I-tositumomab, it can be administered without a loading dose of cold antibody. Humanization allows fractionated injections, and a single-center study demonstrated the feasibility of repeated injections because of the lower immunogenicity of epratuzumab.[7,8]

Different approaches are being explored to improve RIT efficacy in non-Hodgkin lymphoma (NHL): myeloablative RIT or high-dose treatment, RIT as consolidation after chemotherapy, RIT in first-line treatment, and fractionated RIT. In this context, assessing the absorbed dose delivered to the patient is a means to compare treatments delivered via different

**Corresponding author:** Ludovic Ferrer, MS, Medical Physics Department, CLCC Gauducheau, St Herblain, France; Fax: (011) 33 240 67 97 36; l-ferrer@nantes.fnclcc.fr

[1]Medical Physics Department, CLCC Gauducheau, St Herblain, France; [2]INSERM UMR 892, Nantes, France; [3]Nuclear Medicine Department, CLCC Gauducheau, St Herblain, France; [4]Nuclear Medicine Department, University Hospital, Nantes, France; [5]Hematology Department, University Hospital, Nantes, France; [6]Immunomedics, Inc, Morris Plain, New Jersey; [7]Garden State Cancer Center, Center for Molecular Medicine and Immunology, Belleville, New Jersey

The articles in this supplement were presented at the "12th Conference on Cancer Therapy with Antibodies and Immunoconjugates," in Parsippany, New Jersey, October 16-18, 2008.

**Cancer Therapy With Antibodies and Immunoconjugates, Supplement to Cancer.*

**DOI:** 10.1002/cncr.24797, **Received:** June 30, 2009; **Revised:** October 21, 2009; **Published online** February 2, 2010 in Wiley InterScience (www.interscience.wiley.com)

modalities by the use of a common parameter. In addition, the absorbed dose may be used as an index to assess potential toxicity and adapt injected activity and patient follow-up. Dose-limiting toxicity (DLT) of RIT is mostly hematological, depending on the pharmacokinetics of radiolabeled monoclonal antibodies, bone marrow involvement, and prior treatments. Because RIT effects combine radiobiological and immunological mechanisms, the absorbed dose alone may not be sufficient to predict toxicity. In addition, many dosimetric approaches have been proposed thus far, mostly leading to a high variability in the results and an elusive absorbed dose-effect relation. These methods rely on blood-based or image-based approaches.[9-12] Still, some authors reported absorbed dose-toxicity relation in the clinical context of NHL patients.[12]

The aim of this study was to compare the results of red marrow (RM) absorbed dose estimates performed with 3 methods in 5 refractory NHL patients included in an phase 1 and 2 RIT trial assessing fractionated RIT with $^{90}$Y-epratuzumab tetraxetan.

## MATERIALS AND METHODS

### Patients

The respective ethics committees approved the study and all patients gave their informed consent before enrollment. Patients (4 females, 1 male) were enrolled in Nantes (France) as part of a larger, multicenter, phase 1/II dose-escalation study of fractionated RIT with $^{90}$Y-epratuzumab tetraxetan. The study population comprised males or females, ages $\geq$18 years, with histologically confirmed B-cell NHL (any histological grade by REAL classification) who failed after at least 1 regimen of standard chemotherapy and presented with measurable disease by CT, but no single mass with a dimension in any direction greater than 10 cm, and with less than 25% bone marrow involvement. They were at least at 4 weeks beyond any prior chemotherapy, any major surgery, or any radiation therapy. Patients did not received prior external radiation including >25% of the red marrow or exceeding the maximum tolerable levels for critical organs. Patients had adequate performance status (Karnofsky higher than 70%), serum chemistries (serum creatinine lower than 1.5 mg/dl or creatinine clearance higher than 50 mL/min; bilirubin lower than 2 mg/dl) and hematology (hemoglobin higher than 10 g/dL, WBC higher than 3000/mm$^3$, granulocytes higher than 1500/mm$^3$, platelets higher than 100,000/mm$^3$ without transfusions or cytokines for support).

### RIT Administration

Immunomedics, Inc. (Morris Plains, NJ, USA) provided epratuzumab conjugated with the macrocyclic chelating agent, 1,4,7,10-tetra-azacyclodecane-N,N", N"", N"""-tetra-acetic acid (DOTA-epratuzumab), as well as unconjugated epratuzumab. Radiolabeling of DOTA-epratuzumab, purification of the radiolabeled antibody, and immunoreactivity tests were performed as described previously.[7] Patients received 2 co-infusions of 370 MBq/m$^2$ $^{90}$Y-epratuzumab and 120 MBq $^{111}$In-epratuzumab. The 2 co-infusions were administered 1 week apart. Unlabeled epratuzumab was added to achieve a total antibody dose of 1.5 mg/kg/infusion. A conventional clinical, biological and imaging follow-up was performed in the context of clinical study. Hematological toxicity was scored according to the National Cancer Institute Common Toxicity Criteria version 3.0.

### Blood Sampling

After the end of each infusion, 9 blood samples were drawn for pharmacokinetic analyses, usually from between 0.5 hours to 7 days postinfusion. Blood samples were collected in serum-separator tubes, and 0.1 to 0.2 mL of serum was counted for determination of $^{111}$In-activity in a gamma scintillation counter (Minaxi Autogamma 5000; Packard, Meridian, Connecticut), whereas Cerenkov radiation of $^{90}$Y was determined by direct counting in a beta counter (ie, 0.1 mL serum or up to 1.0 mL of urine was placed in saline and counted in a beta counter (Tri-Carb 2100TR; Packard) with a window setting of 0-50 KeV). Scintillation counters were precalibrated against known standards to determine counting efficiencies with automatic background subtraction. Time-activity curves were fit to monoexponentials or biexponentials using gnuplot.[13]

### Imaging Protocol

All whole body (WB) emission scans were performed on a Millennium VG Hawkeye SPECT/CT system with a 1.58-mm-thick NaI(Tl) crystal manufactured by GE Healthcare, and CT scans were performed with the Discovery LS PET/CT system installed in the same nuclear medicine department at Gauducheau Cancer Center (St Herblain, France).

### Attenuation Map Creation

Before the first injection, all patients underwent a whole-body computed tomography (WB CT) scan examination. Because whole-body image acquisition was not possible in 1 step, 2 acquisitions were carried out (5-mm-slice thickness, kVp: 140 kV, 90 mA) head first and feet first, respectively. To obtain the attenuation map, an ImageJ plug-in

was developed to convert pixel content expressed in Hounsfield U into linear attenuation coefficients at the energy of interest for single photon emission computed tomography (SPECT) examination.[14] Despite the finding that $^{111}$In emits 2 gamma rays, we generated only 1 attenuation map at 210 kiloelectronvolts (keV), as suggested by Seo.[15]

Three-dimensional (3D) attenuation maps were projected along the posterior-anterior axis. Resulting pixels of the generated 2D images then contained the attenuation correction factor, as the sum of attenuation coefficients along the direction of projection. Our ImageJ plug-in was then used to concatenate images into a whole-body image (WB) transmission map.

### CT Image Segmentation

We routinely use ITK-SNAP software[16] to label organs of interest such as lungs, liver, spleen, or kidneys. In this work, we used ITK-SNAP to segment trabecular bones present in $L_2$ to $L_4$ vertebrae on CT scans. We developed a program to automatically create 2D regions of interest from individual projection of each segmented volumes. Regions of interest were then used on registered geometric mean images as described below.

### Emission Scans

After each infusion, 5 anterior and posterior WB emission scans were acquired 1 hour postinjection before patient voiding, 4 hours postinjection and at Day 1, 2, and 5. WB scans were acquired in step-and-shoot mode (6 256 × 256 pixels wide frames, duration 5 minutes per frame), using medium energy collimators. This acquisition mode allows only 4 energy windows to be acquired simultaneously (149-155 keV, 159-183 keV, 201-209 keV, 230-264 keV). To correct emission images for scatter, a triple energy window scatter correction method similar to that proposed by Ogawa[17] was implemented. The first to third energy windows were used to create a scatter-corrected image of the 172 keV peak of $^{111}$In. Because detected counts above 264 keV are negligible, the third and fourth energy windows were used to create the second scatter corrected image of the 245 keV peak of $^{111}$In. These 2 calculated scatter-corrected images were then added together. Scatter-corrected anterior and posterior views were used to create a geometric mean (GM) image.

### Image Registration

Scatter-corrected WB GM images were registered against the CT-based WB attenuation correction factor map using an imageJ plug-in developed by Thevenaz.[18] In case of small misalignments between regions of interest and objects in GM images, manual displacements were allowed.

### Activity Scaling and Cumulated Activity Determination

The first imaging session was used to assess camera sensitivity. This factor was calculated as the fraction of $^{111}$In-injected activity over the total counts detected into a WB region of interest (ROI) before any voiding. This factor was supposed to be constant over all the imaging sessions. After correcting for scatter, background, attenuation, and camera sensitivity, the ratio $^{111}$In /$^{90}$Y was used to scale $^{111}$In activity, and differences in physical decay were corrected.

### Red Marrow Dosimetry Assessments

According to the Medical Internal Radiation Dose Committee (MIRD) scheme, the RM dose calculation is expressed as follows:

$$D_{RM} = \tilde{A}_{RM} \times S(RM \leftarrow RM) + \sum_h \tilde{A}_h \times S(RM \leftarrow h) + \tilde{A}_{RB} \times S(RM \leftarrow RB)$$

where $D_{RM}$ is mean absorbed dose to RM. $\tilde{A}_{RM}$ and $\tilde{A}_h$ and $\tilde{A}_{RB}$ are the cumulated activity in RM, other source organs h and the remainder of the body (RB), respectively. $S(RM \leftarrow RM)$, $S(RM \leftarrow h)$, $S(RM \leftarrow RB)$ are the S values from RM, h, and RB to RM. $S(RM \leftarrow RB)$ is given by:

$$S(RM \leftarrow RB) = S(RM \leftarrow TB) \times \frac{m_{TB}}{m_{RB}} - \sum_h S(RM \leftarrow h) \times \frac{m_{TB}}{m_h}$$

where h is organ source excluding RM, $m_{TB}$ is the mass of the total body (TB) and $S(RM \leftarrow TB)$ is the S value from TB to RM.[15]

If there is no specific radiopharmaceutical binding in blood or red marrow, the cumulated activity concentration in blood $C_{blood}$ can be used to assess the activity concentration in red marrow[9] using the red marrow-to-blood ratio (RMBLR),

$$\tilde{A}_{RM} = RMBLR \times C_{blood} \times m_{RM}$$

where $m_{RM}$ equals 1500 g. According to Sgouros,[11] RMBLR depends on the hematocrit (HCT) and is equal

**Table 1.** RM Absorbed Doses and Platelet Toxicity Calculated for Methods M1, M2, and M3

| RM Dose, mGy/MBq | Patient 1 | Patient 2 | Patient 3 | Patient 4 | Patient 5 |
|---|---|---|---|---|---|
| M1 | 4.0 | 4.1 | 2.9 | 4.7 | 8.4 |
| M2 | 2.3 | 2.3 | 2.7 | 2.7 | 2.0 |
| M3 | 2.1 | 2.4 | 2.3 | 2.5 | 1.6 |
| Platelet toxicity | IV | IV | II | IV | IV+++ |
| Leukocyte toxicity | III | III | II | III | IV |

RM indicates red marrow.

to 0.19/(1−HCT), leading to RMBLR = 0.36 for a normal value of HCT. In this study, we called method 2 (M2) the approach where RMBLR is set to a fixed valued of 0.36, and method 3 (M3) the approach where RMBLR depends on the patient's HCT.

These 2 methods cannot take into account any specific radiopharmaceutical uptake in the bone marrow compartment. In fact, according to the inclusion criteria, bone marrow involvement should be ≤25%. A way to assess the dosimetric impact of bone marrow uptake is to use quantitative imaging to derive specific bone marrow uptake as suggested by some authors.[19,20] The image-based method, M1, used the trabecular bone volumes of $L_2$-$L_4$ lumbar spine. This method, in contrast to blood methods M2 and M3, can take into account individual differences in marrow mass. In fact, assuming RM mass in lumbar vertebrae is proportional to trabecular bone volume, RM mass in $L_2$-$L_4$ was calculated by scaling the Reference Man with trabecular bone volume:

$$m^{patient}_{L_2-L_4} = m^{refman}_{L_2-L_4} \times \frac{V^{patient}_{trab\ L_2-L_4}}{V^{refman}_{trab\ L_2-L_4}}$$

where $V^{refman}_{trab}$ $L_2$-$L_4$ is equal to 67 $cm^3$ and $V^{patient}_{trab}$ $L_2$-$L_4$ is the patient's trabecular bone volume calculated during the segmentation process.[20] Then, $\tilde{A}_{RM}$ was calculated by mathematical integration of a monoexponential or biexponential fitting function describing the data points and assuming that the RM mass in $L_2$-$L_4$ is 6.7% of the total RM mass.[20]

Hence,

$$D_{RM} = \frac{\tilde{A}_{L_2-L_4}}{0.067} \times S(RM \leftarrow RM) \times \frac{V^{refman}_{trab\ L_2-L_4}}{V^{patient}_{trab\ L_2-L_4}}$$

where $S(RM \leftarrow RM)$ is taken from MIRD pamphlet 11.[21]

## RESULTS

Table 1 summarizes platelet and leukocyte toxicities. Patient 3 showed a mild hematological toxicity, with only grade 2 toxicity for platelets and leukocytes. A higher hematological toxicity was observed in the Patients 1, 2 and 4, with a grade 4 thrombocytopenia and a grade 3 leukopenia, of usual duration. Patient 5 showed a prolonged grade 4 toxicity for both platelets and leukocytes, requiring a stem cell graft. This severe toxicity could be explained by a transformation of a low-grade lymphoma and a progression in bone marrow between patient inclusion and treatment.

Figure 1 shows the posterior view from the fast WB scans, used to illustrate the biodistribution of $^{111}$In-epratuzumab, 1 hour postinjection. Blood pool activity is the most prominent feature, with activity in the heart, large pulmonary vessels, major blood vessels, vertebrae, liver, spleen, and kidneys. The bladder was also usually observed on the 1-hour, prevoiding view. The spine uptake was different among the 5 patients. In 3 of the 5 patients (1,3,4), the observation of the lumbar vertebrae was low, whereas 2 patients (2,5) presented a more intense lumbar spine uptake, with individual vertebrae clearly delineated from each other. Figure 1 also shows lumbar regions of interest used to calculate RM-absorbed doses by method M1. Figure 2 shows patient posterior views acquired 7 days after $^{111}$In-epratuzumab injection. Patient 5 had a more intense sacrum and lumbar uptake than Patient 2.

Table 1 summarizes RM-absorbed doses for the 2 infusions calculated by the 3 different methods M1, M2, and M3. With M2, the median value was 2.3 mGy/MBq, ranging from 2.0 (in Patient 5) and 2.7 in Patient 4. With M3, the median value was 2.3 mGy/MBq, ranging from 1.6 (in Patient 5) and 2.5 in Patient 4. The method M1, including imaging, seemed to provide the best absorbed dose-effect relation. Method M1 showed higher red marrow results in 4 patients. The median value was 4.0 mGy/MBq, ranging from 2.9 (in Patient 3) and 8.4 in Patient 5. The 4 patients with the highest RM-absorbed doses

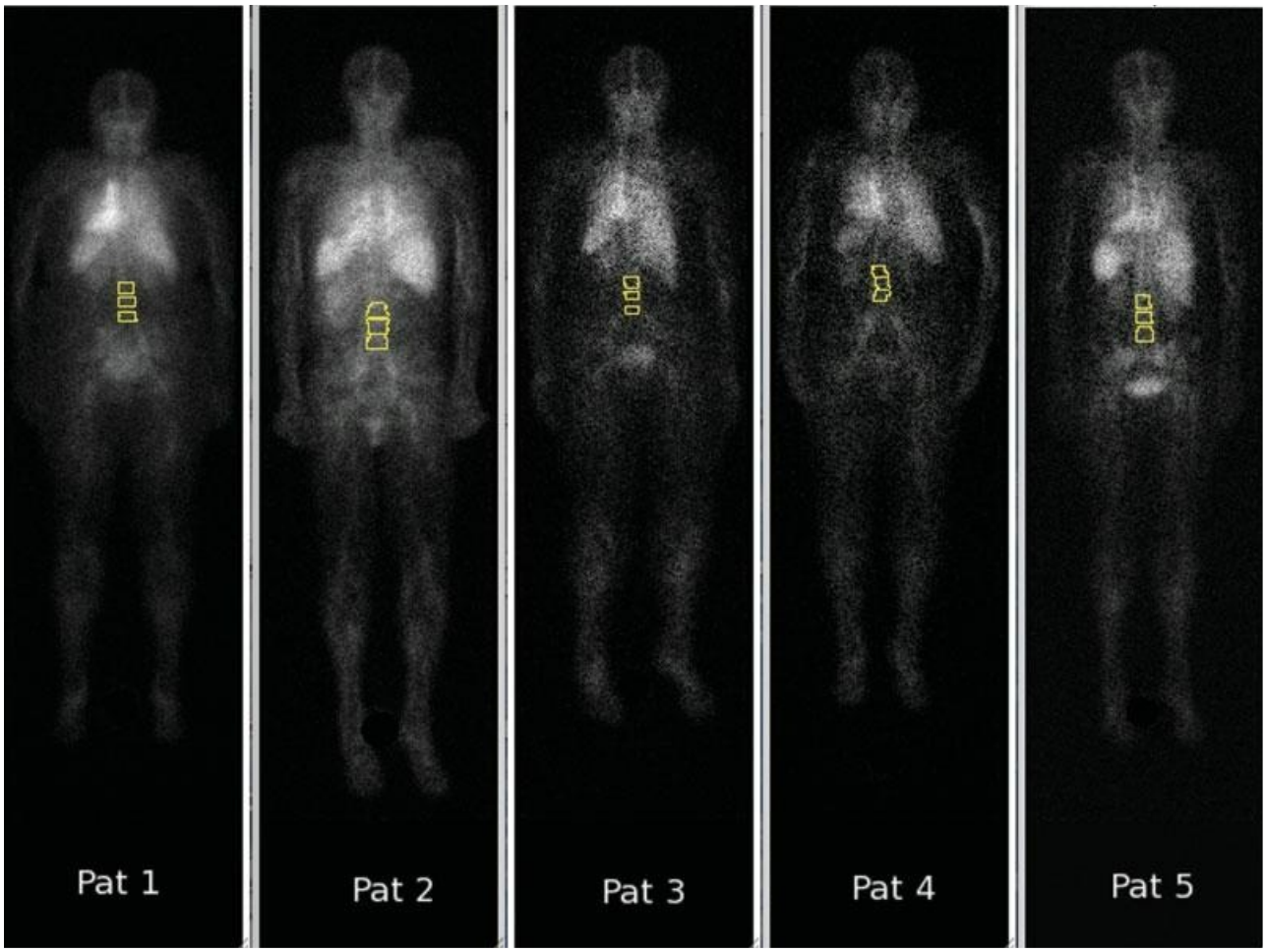


**Figure 1.** Posterior views were recorded 1 hour after injection of $^{111}$In-epratuzumab. The images show the different bone marrow uptake observed in the 5 patients: Patients 2 and 5 presented a more intense lumbar spine uptake. Lumbar regions of interest derived from L2-L4 segmentation are shown.

showed grade 4 toxicity; Patient 5 had much more severe toxicity, requiring stem cell transplantation. Patient 3, with the lowest absorbed dose, showed only mild (grade 2) toxicity. As can be seen in Table 2, RM effective half-life were very similar between first and second infusion.

## DISCUSSION

In this study, 3 different approaches were used to derive bone marrow-absorbed dose in 5 NHL patients undergoing RIT. As suggested in previous studies, image-based methodology (M1) seems to better predict hematological toxicity as compared with blood-based methods in NHL patients.[22] Despite the reduced number of patients, some preliminary conclusions can be drawn.

Blood-based approaches (M2 and M3) are obviously easier to implement in practice. They require only blood sampling at various time points after radiopharmaceutical injection, and a patient-specific determination of the hematocrit for M3. Inclusion criteria included a bone marrow involvement lower than 25%. In that respect, using M2 or M3 could be justified under the hypothesis that less than 25% of bone marrow involvement has no significant dosimetric consequence on bone marrow. However, the bone marrow involvement was assessed using iliac crest bone marrow biopsy, and iliac crest bone marrow biopsy is associated with a high rate of false-negative results.

In contrast, the image-based approach M1 is methodologically much more demanding. It requires a preliminary $^{111}$In-labeled radiopharmaceutical injection, several imaging sessions, and the implementation of ad hoc image/data processing. In addition, it adds to the burden of the patient who has to undergo additional examinations and is more costly in terms of hospital resource requirements.

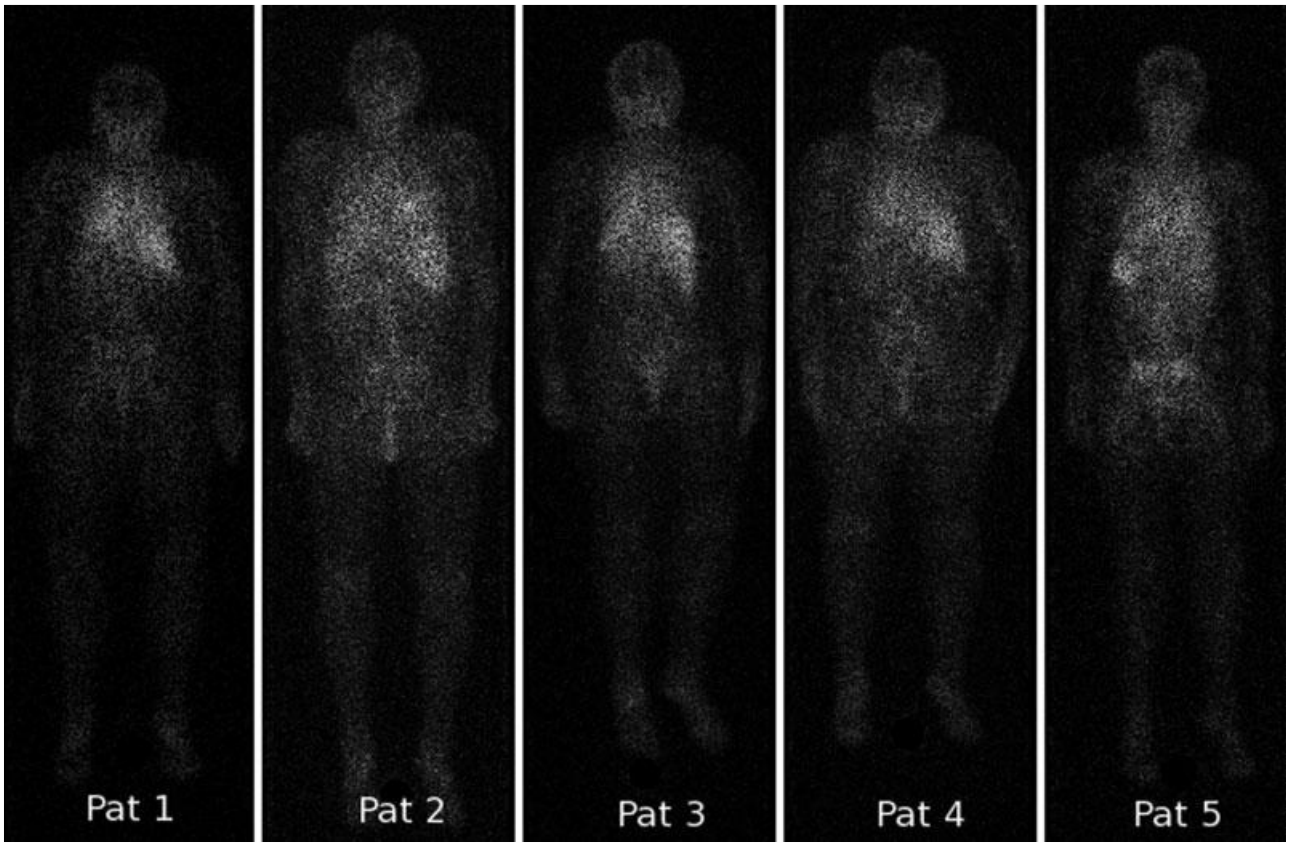


**Figure 2.** Posterior views were recorded 7 days after injection of $^{111}$In-epratuzumab. Patient 5 showed the most intense sacrum and lumbar uptake.

**Table 2.** Patient RM Effective Half-Life Calculated for the Method M1

| Effective Half-Life, h | Patient 1 | Patient 2 | Patient 3 | Patient 4 | Patient 5 |
|---|---|---|---|---|---|
| Infusion 1 | 62 | 63 | 60 | 55 | 61 |
| Infusion 2 | 63 | 61 | 61 | 58 | 59 |

The accuracy of absorbed dose calculations is always a subject of debate. From that perspective, M2 and M3 have the clear advantage, requiring much less data processing, and, therefore, results can be obtained with a fairly improved confidence as compared with absorbed dose calculations derived from M1; M2 and M3 require only a properly calibrated scintillation counter (to get $C_{Blood}$) and HCT determination (for RMBLR). Siegel and colleagues[23] questioned the use of HCT. First of all, the 0.19 value was used to derive RMBLR results from a preclinical assessment in rabbit femur and was not meant to be applied to patients whose marrow may have been compromised by previous therapy. In addition, some clinical studies[12] found no difference in RM dose estimations obtained from a fixed (0.32) and HCT-adjusted RMBLR values. Obviously, blood sampling times and curve fitting algorithms used to derive $C_{Blood}$ will have an impact on the result, but the main issue in this approach is that it considers a fixed bone marrow mass (1500 g) for each patient. Using a patient-specific bone marrow mass would certainly increase the degree of confidence in the results obtained in methods M2 and M3. Still, these methods provide for an index that can be used for comparing studies performed in different centers, using different radiopharmaceuticals or administration schemes. Because blood-based approaches disregard any bone marrow involvement, they can also be considered as the minimum absorbed dose delivered to patient bone marrow, although this statement is also subject to debate.

Image-based approaches suggest the implementation of a much more refined data processing protocol. With all possible care taken in processing the acquired data, the number of operator-dependant steps intrinsically limits the reproducibility of the approach (independently of the accuracy). Absorbed doses generated using M1 should, therefore, be taken as a relevant index to compare the irradiation delivered to patients, while keeping in mind that the absolute numbers (Gy) given should be considered with caution.

That being said, the dosimetric results obtained in this work are striking despite the low number of patients studied: M2 and M3 essentially lead to the same results, with an equivalent median of 2.3 mGy/MBq, and a relatively low variation around this figure (range, 1.6 to 2.7 mGy/MBq). These results, when put in front of the observed toxicity, show no correlation at all. In fact, Patient 5 who exhibited the more severe toxicity has had the lower absorbed dose as determined by M2 (2.0 mGy/MBq) or M3 (1.6 mGy/MBq).

M1, in contrast, seem to provide for a good toxicity index: The lower absorbed dose (2.9 mGy/MBq) corresponded to the mildest toxicity (grade 2) in Patient 3, whereas the highest absorbed dose (8.4 mGy/MBq) was obtained for the patient who suffered from the more severe toxicity (prolonged grade 4 toxicity for both platelets and leukocytes, requiring a stem cell graft, Patient 5). The remaining 3 patients (Patients 1, 2, and 4) had a severe grade 3 (leukocyte) and grade 4 (platelet) toxicity, with an absorbed dose between 4.0 and 4.7 mGy/MBq.

As was stated previously, the absorbed doses computed using an image-based approach should be interpreted cautiously. The median-absorbed dose computed using approach M1 was almost double that obtained with M2 and M3 (4.1 vs 2.3 and 2.3 mGy/MBq, respectively). Because of possible improvements that could be brought to the various approaches (patient-specific bone marrow mass for M2 and M3, or optimized activity determination protocol for M1), the ratio of blood-only to image-based absorbed dose determinations may vary in the future. Still, it must be stressed that at this stage and for the limited number of patient studied here, only the image-based approach seems to be predictive of the observed toxicity. This in agreement with results presented previously by other groups.[22]

### *Conclusion/Perspectives*

Although few patients were enrolled in this study, this work showed that imaging-based dosimetry for RM seems to give better dose-toxicity correlation, as already suggested by different authors.[23-25] Our study suggests that even for patients with a low BM involvement (<25%), it is important to take into account the radiopharmaceutical uptake in BM. This is especially relevant within the context of $^{90}$Y-labeled radiopharmaceuticals, because long-range beta particle irradiation may enhance BM toxicity because of targeted cancer cells located in the neighborhood of normal hematopoietic cells. However, the high RM-absorbed doses observed in this study with image-based dosimetry suggest potential improvements. Image-based dosimetry protocol highly relies on the correction of background activity present in underlying or overlying tissues. For example, to better take into account the contribution of the activity in large blood vessels near lumbar spines, one could use the approach described by Meredith.[26] In addition, because all patients underwent whole-body computed-tomography scans, we could advantageously use the CT-assisted matrix inversion method.[27]

The characterization of the absorbed dose-effect relation is a matter of high importance within the context of targeted radionuclide therapy, to increase the quality of the delivered treatment. Still, the absorbed dose alone may not be sufficient to fully characterize the observed toxicity, especially for previously treated patients. First-line targeted radionuclide therapy protocols, ie, involving patients naïve to any other form of treatment, may provide important information in this domain. Another aspect to consider, in addition of the absorbed dose, is the impact of the absorbed dose rate, fractionation, sensitivity of irradiated tissues, ie, radiobiological parameters, as recently suggested by Wessels et al to derive kidney toxicity in radionuclide therapy.[28]

## CONFLICT OF INTEREST DISCLOSURES

The articles in this supplement represent proceedings of the "12th Conference on Cancer Therapy with Antibodies and Immunoconjugates," in Parsippany, New Jersey, October 16-18, 2008. Unrestricted grant support for the conference was provided by Actinium Pharmaceuticals, Inc., Bayer Schering Pharma, Center for Molecular Medicine and Immunology, ImClone Systems Corporation, MDS Nordion, National Cancer Institute, NIH, New Jersey Commission on Cancer Research, and PerkinElmer Life & Analytical Sciences. The supplement was supported by an unrestricted educational grant from ImClone Systems Corporation, a wholly owned subsidiary of Eli Lilly and Company, and by page charges to the authors.

## REFERENCES

1. Goldenberg DM, Sharkey RM. Advances in cancer therapy with radiolabeled monoclonal antibodies. *Q J Nucl Med Mol Imaging.* 2006;50:248-264.

2. Chatal JF. Radioimmunotherapy, a new breakthrough in the treatment of follicular non-Hodgkin's lymphoma: the European perspective. *Cancer Biother Radiopharm.* 2006;21: 1-4.
3. Goldenberg DM, Horowitz JA, Sharkey RM, et al. Targeting, dosimetry, and radioimmunotherapy of B-cell lymphomas with iodine-131-labeled LL2 monoclonal antibody. *J Clin Oncol.* 1991;9:548-564.
4. Juweid M, Sharkey RM, Markowitz A, et al. Treatment of non-Hodgkin's lymphoma with radiolabeled murine, chimeric, or humanized LL2, an anti-CD22 monoclonal antibody. *Cancer Res.* 1995;55:5899s-5907s.
5. Juweid M, Stadtmauer E, Sharkey RM, et al. Pharmacokinetics, dosimetry and initial therapeutic results with $^{131}$I- and $^{111}$In-/$^{90}$Y-labeled humanized LL2 anti-CD22 monoclonal antibody in patients with relapsed/refractory non-Hodgkin's lymphoma (NHL). *Clin Cancer Res.* 1999;5: 3292s-3303s.
6. Sharkey RM, Brenner A, Burton J, et al. Radioimmunotherapy of non-Hodgkin's lymphoma with $^{90}$Y-DOTA humanized anti- CD22 IgG ($^{90}$Y-epratuzumab): do tumor targeting and dosimetry predict therapeutic response? *J Nucl Med.* 2003;44:2000-2018.
7. Linden O, Hindorf C, Cavalin-Stahl E, et al. Dose-fractionated radioimmunotherapy in non-Hodgkin's lymphoma using DOTA-conjugated, $^{90}$Y-radiolabeled, humanized anti-CD22 monoclonal antibody, epratuzumab. *Clin Cancer Res.* 2005;11:5215-5222.
8. Griffiths GL, Govindan SV, Sharkey RM, Fisher DR, Goldenberg DM. $^{90}$Y-DOTA-epratuzumab: An agent for radioimmunotherapy of non-Hodgkin's lymphoma. *J Nucl Med.* 2003;44:77-84.
9. Siegel JA, Wessels BW, Watson EE, et al. Bone marrow dosimetry and toxicity for radioimmunotherapy. *Antibodies Immunoconjugates Radioimmunopharm.* 1990;3:213-233.
10. Shen S, DeNardo GL, Sgouros G, O'Donnell RT, DeNardo SJ. Practical determination of patient-specific marrow dose using radioactivity concentration in blood and body. *J Nucl Med.* 1999;40:2102-2106.
11. Sgouros G. Bone marrow dosimetry for radioimmunotherapy: theoretical considerations. *J Nucl Med.* 1993;34:689-694.
12. Siegel JA, Yeldell D, Goldenberg DM, et al. Red marrow radiation dose adjustment using plasma FLT3-L cytokine levels: Improved correlations between hematologic toxicity and bone marrow dose for radioimmunotherapy patients. *J Nucl Med.* 2003;44:67-76.
13. Williams T, Kelley C. Available at: http://www.gnuplot.info. Accessed February 18, 2009.
14. Ferrer L, Carlier T, Lisbona A, Bardies M. An ImageJ plugin to create WB TAC using CT scanner. *Eur. J Nucl Med.* 2007;34(suppl):S198.
15. Seo Y, Wong KH, Sun M, Franc BL, Hawkins RA, Hasegawa BH. Correction of photon attenuation and collimator response for a body-contouring spect/ct imaging system. *J Nucl Med.* 2005;46:868-877.
16. Yushkevich PA, Piven J, Hazlett HC, et al. User-guided 3D active contour segmentation of anatomical structures: Significantly improved efficiency and reliability. *Neuroimage.* 2006;31:1116-1128.
17. Ogawa K, Harata Y, Ichihara T, Kubo A, Hashimoto SA. Practical method for position-dependent compton-scatter correction in single photon emission ct. *IEEE Trans Med Imaging.* 1991;10:408-412.
18. Thevenaz P, Ruttimann UE, Unser MA. Pyramid approach to subpixel registration based on intensity. *IEEE Trans Image Process.* 1998;7:27-41.
19. Siegel JA, Lee RE, Pawlyk DA, Horowitz JA, Sharkey RM, Goldenberg DM. Sacral scintigraphy for bone marrow dosimetry in radioimmunotherapy. *Int J Rad Appl Instrum B.* 1989;16:553-559.
20. Shen S, Meredith RF, Duan J, et al. Improved prediction of myelotoxicity using a patient-specific imaging dose estimate for non-marrow-targeting y-antibody therapy. *J Nucl Med.* 2002;43:1245-1253.
21. Feller PA, Sodd VJ, Kereiakes JG. Using the S tables of MIRD Pamphlet 11. *J Nucl Med.* 1977;18:747.
22. Juweid M, Sharkey RM, Siegel JA, Behr T, Goldenberg DM. Estimates of red marrow dose by sacral scintigraphy in radioimmunotherapy patients having non-Hodgkin's lymphoma and diffuse bone marrow uptake. *Cancer Res.* 1995;55:5827s-5831s.
23. Siegel JA. Establishing a clinically meaningful predictive model of hematologic toxicity in nonmyeloablative targeted radiotherapy: practical aspects and limitations of red marrow dosimetry. *Cancer Biother Radiopharm.* 2005;20:126-140.
24. Lim SM, DeNardo GL, DeNardo DA, et al. Prediction of myelotoxicity using radiation doses to marrow from body, blood and marrow sources. *J Nucl Med.* 1997;38:1374-1378.
25. DeNardo DA, DeNardo GL, O'Donnell RT, et al. Imaging for improved prediction of myelotoxicity after radioimmunotherapy. *Cancer*. 1997;80:2558s-2566s.
26. Meredith RF, Shen S, Forero A, LoBuglio AF. A method to correct for radioactivity in large vessels that overlap the spine in imaging-based marrow dosimetry of lumbar vertebrae. *J Nucl Med.* 2008;49:279-284.
27. Liu A, Williams LE, Raubitschek AA. A CT assisted method for absolute quantitation of internal radioactivity. *Med Phys.* 1996;23:1919-1928.
28. Wessels BW, Konijnenberg MW, Dale RG, et al. MIRD pamphlet no. 20: The effect of model assumptions on kidney dosimetry and response–implications for radionuclide therapy. *J Nucl Med.* 2008;49:1884-1899.